

CHARACTERISTICS OF FRACTURE SURFACE AND FATIGUE RESISTANCE IN ASTM A36 STEEL PRESSURE VESSEL MATERIAL

Ikbal Azhari¹⁾, Hendri Chandra^{1)*}, Ozkar F. Homzah², Tri Satya Ramadhoni², Rachmat Dwi Sampurno²

¹⁾ Department of Mechanical Engineering, Universitas Sriwijaya, Jl. Raya Palembang-Prabumulih KM. 32 Inderalaya Ogan Ilir Ol South Sumatera

²⁾ Department of Mechanical Engineering, Politeknik Negeri Sriwijaya, Jl. Sriwijaya Negara, Bukit Besar, Palembang - Indonesia

* Corresponding email: hendrichandra@ft.unsri.ac.id

ARTICLE INFORMATION

Revised
17/03/2024

Accepted
02/05/2024

Online Publication
31/05/2024

©2024 The Authors. Published by
AUSTENIT (Indexed in SINTA)

doi:

[10.53893/austenit.v16i1.7219](https://doi.org/10.53893/austenit.v16i1.7219)

ABSTRACT

Pressure vessels are equipment in the industrial field to hold pressurized fluids, such as gas, oil and chemicals, ASTM A36 steel is one type of material that can be used in pressure vessels, this steel has good mechanical properties but still has limitations in its fatigue resistance. Pressure vessels receive internal and external loads, this pressure difference results in stress on the wall (shell). This stress can cause material damage, therefore the author conducted fatigue repeated bending and Scanning electron microscopy (SEM) testing to analyze fatigue resistance and fracture surface characteristics. Fatigue testing of 4 specimens with angle variations of 4°, 8°, 11° and 13° resulted in a cycle count of 1490200 cycles, 400050 cycles, 234200 cycles and 99000 cycles respectively. SEM results of the fracture surface of the 4° and 13° testing angles of ASTM A36 steel showed striation and microvoid coalescence and crack propagation indicating that the fatigue failure that occurred was ductile fracture. Based on the conclusions obtained, it shows that the number of cycles is influenced by the testing stress, which means that at high stresses, the life time of the pressure vessel will be smaller and vice versa.

Keywords : pressure vessel, ASTM A36 steel, fatigue, scanning electron microscopy (SEM)

1 INTRODUCTION

The pressure vessel is one of the equipment used in the industrial field as a container for pressurized fluids such as chemicals, oil, and gas. Pressure vessels receive internal (temperature, volume, or amount of gas) and external (temperature, altitude, atmospheric pressure or weather conditions) loads (Nugraha et al., 2022). The pressure difference between the inside and outside results in stress on the vessel wall (shell) that increases with the difference in pressure and radius of the vessel (Moss & Basic, 2013). This stress results in plastic deformation or a permanent change in the shape of the material because the stress exceeds the elastic limit. While the stress distribution of a thick-walled pressure vessel varies across the section, a thin-walled pressure vessel for pressure analysis is considered uniform because the difference between the inside and outside surfaces is small (Siswanto et al., 2021). The fluid in the pressure vessel will be hazardous for the surrounding environment and worker safety when a failure occurs in the design or manufacture of

pressure vessels based on division II standards (ASME, 2015) for pressure vessel material selection and division VIII standards (ASME, 2019) for pressure vessel technical codes and standards

ASTM A36 steel is one type of carbon steel with low carbon content used in industrial fields such as oil, gas or chemicals. Low carbon steel contains between (0.025%-0.25%) C, and each ton of low carbon steel contains 10-30 kg of carbon (Wiryosumarto & Okumura, 2000). Increasing the carbon content and other alloying elements will increase the mechanical properties of carbon steel, but this has the effect of increasing the price of the material (ASTM, 2008). ASTM A36 steel has good mechanical properties but is still prone to fatigue failure. ASTM A36 steel can be used for a wide variety of applications, depending on the thickness of the plate and also the level of corrosion resistance (Humaidi et al., 2022).

The surface fracture characteristic of a material indicates the physical and morphological properties of the surface formed by the fracture process. The surface fracture characteristics in various types of fractured materials such as ductile

fracture, brittle fracture, fatigue fracture, and overload fracture (Megyesy, 2008). Ductile fracture material undergoes plastic deformation before finally breaking, its characteristics show cracks, extensive deformation, and clear plastic region (Wciślik & Lipiec, 2022). Brittle fracture materials fracture without significant plastic deformation and very quickly, characterized by transverse cracks and no obvious plastic deformation (Pineau et al., 2016). Fatigue fracture of materials subjected to repeated or fluctuating loads, characterized by early cracks, benchmarks, and striations. Overload fracture of materials subjected to loads exceeding their strength limit and fracturing rapidly and without prior deformation, characterized by rough and irregular surfaces (Chandra et al., 2024).

The most common failure due to machines use is fatigue failure (Schneller et al., 2022). ASTM A36 steel is a type of material for pressure vessels subjected to repeated loads due to internal pressure. This steel has limitations in its fatigue resistance. Therefore, the author conducted fatigue testing using the repeated bending method to analyze the fatigue resistance of the material.

2. MATERIALS AND METHODS

The ASTM A36 steel is one of the materials used to manufacture thin cylinder pressure vessels. Based on (the mill certificate) ASTM A36 steel has a chemical composition and mechanical properties as seen in Table 1 and Table 2 below:

Table 1. Chemical composition of ASTM A36 steel (Mill Certificate)

No	Chemical composition	wt.%
1	Carbon (C)	0.20
2	Silicon (Si)	0.24
3	Manganese (Mn)	1.067
4	Phosphorus (P)	0.025
5	Sulfur (S)	0.024

Table 2. Mechanical properties of ASTM A36 steel (Mill Certificate)

No	Mechanical Properties	Value
1	Yield Strength (MPa)	245 – 300
2	Ultimate Tensile Strength (MPa)	420 – 440
3	Elongation (%)	27 – 30

Manufacture of flat plate specimens for repeated bending fatigue testing in the Mechanical Engineering workshop of SMK Negeri 2 Palembang based on the machine manual book, with dimensions of length, width, and height (5×20×90) mm, as shown in Figure 3.2 below.

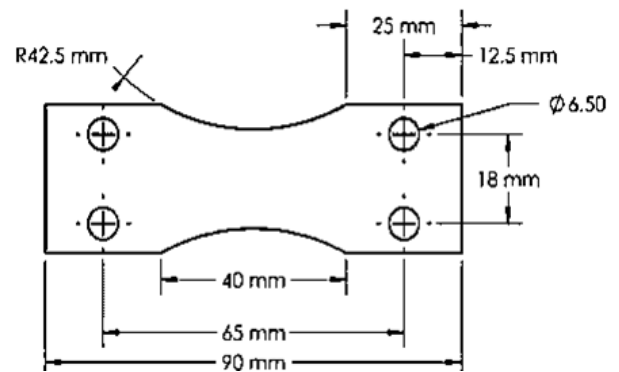


Figure 1 . Dimension of fatigue repeated bending test specimen

2.1 Testing Method

The tests and observations used in this final project research are as follows.

2.2.1 Repeated bending fatigue testing

Repeated bending fatigue testing to determine the fatigue resistance value of the material based on the JIS Z 2273 General Rules for Fatigue Testing of Metal standard, using Torsee's Repeated Torsion & Bending Fatigue Testing Machine type FTS-4, at the Sriwijaya University Mechanical Engineering Materials Laboratory.

Table 3. The specifications of the fatigue testing machine in the Materials Laboratory

No	Parameter	Value
1	Tool model	FTS-4
2	Maximum torsion angle	$\pm 15^\circ$
3	Motor rotation	3.000 rpm
4	Static load	± 2 kgf.m
5	Sulfur	2 kgf.m
6	Effective distance between hooks	50-220 mm

2.2.1 Repeated bending fatigue testing

Visual inspection of the surface aims to detect the presence of cracks, scratches, or other defects on the surface of the material. Inspection methods can be performed using the naked eye, the use of reflective light, or the use of microscopic observation equipment.

2.2.3 Metallography/microstructure testing

Metallography is a method of studying the microstructure of solid materials, which are processed by staining, etching, and polishing techniques. Through this examination, researchers can identify various characteristics, such as grain size and shape and the presence of defects and other mechanical properties.

2.2.4 Scanning electron microscopy (SEM)

One of the solid material testing techniques to observe the surface structure of materials using electron beam. SEM can magnify three-dimensional surfaces up to thousands of times and to know the microstructure specimens (Darmo et al., 2018). In this test, the sample is placed in a vacuum tube, then shot with an electron beam, reflected from the surface of the material, and then taken and processed into an image using special software. SEM is used to study the structure and morphology of surfaces, wear, corrosion, and fractures in materials.

3. RESULTS AND DISCUSSION

3.1 Fatigue Testing Results

Based on Table 4, the testing angle is directly proportional to the stress and inversely proportional to the time or number of cycles, which means that the greater the testing angle or stress, the smaller the time or number of material cycles will be.

Table 4 . ASTM A36 steel fatigue test result data

No	Parameter	Value			
1	Angles	4°	8°	11°	13°
2	Time (s)	29804	8001	4684	1980
3	Rotation (rps)	50	50	50	50
4	Cycle	149020 0	400050	234200	9900 0
5	Stress (MPa)	62.77	125.54	172.62	204.0 1

This is because the greater the stress, the greater the load and vibration the specimen receives, making the specimen break faster.

$$Cycle (N) = t \times n \tag{1}$$

$$Moment\ of\ Inertia\ (I) = \frac{[bh]^3}{12} \tag{2}$$

$$Bending\ moment\ (M) = (\theta/\theta_{max}) \times \tau \tag{3}$$

$$Bending\ stress\ (\sigma_b) = (M \times y)/I \tag{4}$$

3.2 S-N Curve

Based on the data from the calculation of the fatigue repeated bending test of ASTM A36 steel at test angles 4°, 8°, 11°, and 13°, the S-N curve (the relationship between stress S and the number of cycles N) is obtained as shown in Figure 2, the number of cycles is inversely proportional to the stress which means that the number of cycles will decrease if the stress increases, from the S-N curve the fatigue resistance value of the ASTM A36 steel specimen is obtained which is at a lower stress than 62.77 MPa, this is because the S-N curve has not flattened or the number of cycles at that stress has not approached infinity. Fatigue limit is the ability of

the material to accept fatigue loads where an unlimited number of cycles can be endured by the material without failure (Hafidz & Chandra, 2023).

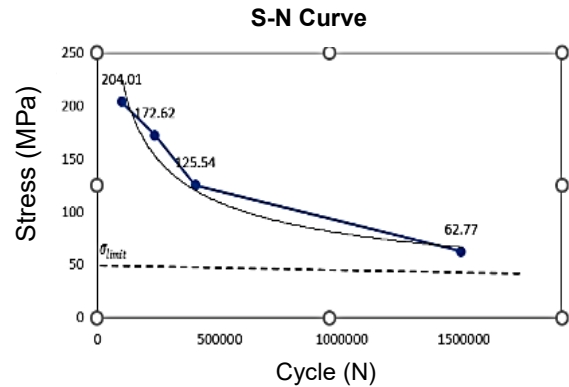


Figure 2. S-N Curve

3.3 Macro Structure

Repeated bending fatigue testing with Torse's Repeated Torsion & Bending Fatigue Testing Machine type FTS-4 with a stress ratio (R=0), the maximum amplitude stress (Smax) has a value of zero, so only the minimum amplitude stress (Smin) applies. It can be seen from the movement of the specimen anvil, which moves down (negative position) towards the neutral position (zero), as shown in Figure 3.



Figure 3. Fatigue repeated bending loading position

The formation of beachmarks or striations is strongly influenced by stress, type of loading and stress ratio (R). beachmarks will be more regular and visible to the eye if the stress ratio (R = -1) or minimum stress is equal to the minimum stress. Stress affects the beachmark or crack propagation, which means that the smaller the stress in the material, the wider the beachmark on the fracture surface and vice versa. However, even though this final project research uses a stress ratio (R=0) it does not reduce the evidence of fatigue fracture surfaces with indications such as beachmarks or striations that can only be seen with SEM (Chandra, 2019).

The results of observations with a PME 3 11B optical microscope at the Sriwijaya University Materials Laboratory show the initial crack, crack propagation with a benchmark, and, in the end, a break in the specimen. Crack initiation at the bottom or top of the specimen and the center of the specimen is neutral; the cause is on the uneven surface of the specimen, so the stress experienced by the specimen surface is uneven, and the fracture is irregular. Based on previous research to flatten the surface of ASTM A36 steel using the MITSUBISHI CNC-Mill A3 machine using feeders

(0.15, 0.1, and 0.05) mm, it was concluded that the smaller the feed on the workpiece, the higher the percentage of surface flatness (Suryana et al., 2015).

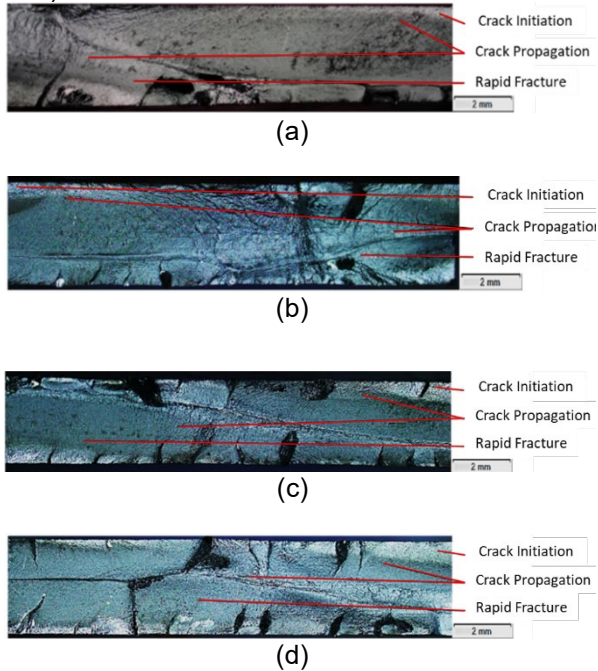


Figure 4. Fatigue fracture surface of ASTM A36 steel testing angle (a) 4°; (b) 8°; (c) 11°; (d) 13°.

Failure due to fatigue begins with cracks on the surface of the specimen, this proves that fatigue properties are very sensitive to surface conditions, such as roughness, residual stress and changes in surface properties (Pratowo & Apriansyah, 2016). In Figure 4 the benchmark or crack propagation area tends to be wider at the smallest test angle (4°) and narrower at the largest test angle (13°), the angle is directly proportional to the working stress, which means that the smaller the angle or test stress, the wider the crack propagation area and vice versa.

3.4 Micro Structure

Observation of the microstructure or metallography of the Materials Engineering Laboratory of Sriwijaya University, as seen in Figure 5, shows that ASTM A36 steel is a low-carbon steel with a carbon composition of 0.20%.

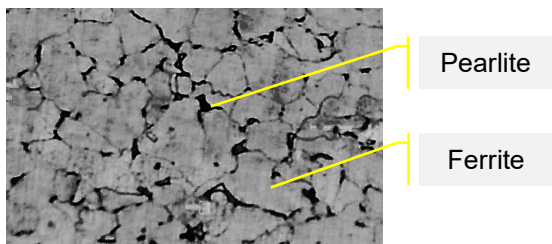


Figure 5. Metallographic results of ASTM A36 steel 450x magnification scale

Figure 5 shows that the phase formed is ferrite-pearlite, with a ferrite fraction value of 77.42% and pearlite 22.58%. The number of

pearlite grains indicates the carbon content of the steel; the fewer pearlite grains are seen, the lower the carbon content.

3.5 Scanning electron microscopy (SEM)

Scanning electron microscopy is one of the solid material testing techniques to observe the 3D surface structure of materials using an electron beam with a high magnification scale. The results of SEM observations on the fracture surface of ASTM A36 steel at testing angles of 4° and 13° are shown in Figures 6 and 7.

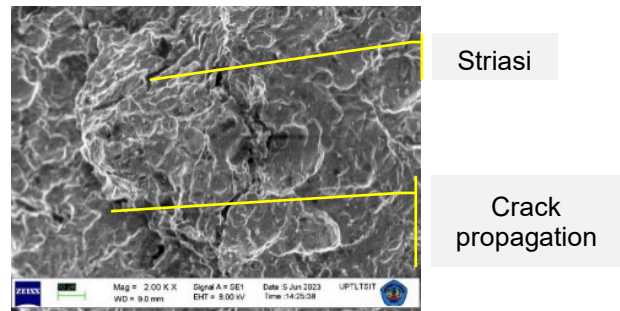


Figure 6. SEM results on the fatigue fracture surface of ASTM A36 steel at a testing angle of 4° with a magnification scale of 2000x

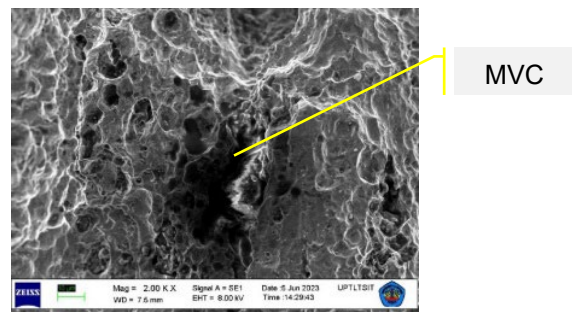


Figure 7. SEM results on the fatigue fracture surface of ASTM A36 steel at a testing angle of 13° with a magnification scale of 2000x

According to (H. O. Fuchs & Stephens, 1980), Scanning electron microscopy (SEM) analysis of fatigue crack growth mechanisms, there are three common modes such as striation formation, Microvoid coalescence and Micro Cleavage (Bharati et al., 2024). Striation is the pattern of stripes seen in fatigue fractures, when the material is subjected to repeated load cycles small cracks occur which eventually lead to the final fracture. Striations are traces of small cracks that look like lines arranged in a repetitive manner on the surface of the fracture. Microvoid coalescence (MVC) is a phenomenon that occurs in ductile materials during plastic deformation, when the material undergoes load cycles small spaces (Microvoids) are formed, during continuous deformation the small spaces coalesce to form larger voids or coalescence of other cracks. Micro Cleavage (MC) is a type of deformation that occurs in brittle materials, small fragments will occur on a

microscopic scale, MC is often seen under rapid and sharp loads such as ceramics or glass (Li et al., 2023).

SEM results show that the fracture surface of the material displays striations and microvoid coalescence. A single beachmark can contain thousands of striations, each 1 striation representing one cycle of crack growth, often striations are scattered throughout the fracture surface and may not be obvious due to friction or pounding of the material surface during repeated loading.

In the results of fatigue testing cycle and stress calculations, the testing angle is directly proportional to the stress and inversely proportional to the number of cycles, which means that the greater the testing angle, the smaller the number of cycles, this can be seen in table 4.2 of ASTM A36 steel fatigue testing data. On visual observation, the difference occurs in crack propagation, whereas in specimens with a 4° testing angle, the crack propagation area tends to be wider compared to specimens given an angle of 8°, 11°, and 13°. This is due to the larger testing angle, the load and vibration received by the specimen will be greater and cause the fracture process in the specimen to be faster.

Metallographic observation or microstructure of ASTM A36 steel shows that the phase formed is ferrite-pearlite. The value of the ferrite fraction is 77.42% and the pearlite fraction is 22.58%, the number of pearlite grains indicates the carbon content contained in the material, ASTM A36 steel includes low carbon steel with levels of 0.20 C%.

Scanning electron microscopy (SEM) results on two specimens from fatigue repeated bending testing at angles of 4° and 13° show that there are striations that are part of the beachmark (on one coastline or beachmark there are thousands of striations), crack propagation, and microvoid coalescence found in ductile materials. This indicates that the fracture that occurs in this fatigue test is a fatigue fracture indicated by the presence of striations and MVC.

4 CONCLUSIONS

The conclusion obtained from this study shows that the fatigue limit of ASTM A36 steel is at a stress lower than 62.77 MPa. This is because the number of cycles on the S-N curve has not approached infinity. The fatigue test results show that the number of cycles is inversely proportional to the testing angle, the greater the testing angle, the smaller the number of cycles. Visual observation shows that the crack propagation is smoother and longer at low test angles and vice versa. Microstructure observation shows a ferrite-pearlite phase, with a ferrite fraction value of 77.42% and pearlite of 22.58%. SEM results of the fracture surface of the 4° and 13° testing angles of ASTM

A36 steel showed striation, microvoid coalescence, and crack propagation, indicating that the fatigue failure was a ductile fracture.

REFERENCES

- ASME. (2015). *SECTION II Part A Ferrous Material Specifications (SA-451 to End) 2015 ASME Boiler and Pressure Vessel Code An International Code*.
- ASME. (2019). *SECTION VIII Rules for Construction of Pressure Vessels 2019 ASME Boiler and Pressure Vessel Code An International Code*. <https://www.asme.org/shop/certification-accreditation>.
- ASTM. (2008). *Standard Specification for Carbon Structural Steel*. www.astm.org.
- Bharati, M., Maity, R., Singh, A., & Paul, S. K. (2024). The fatigue crack growth behavior of hydrogenated 9Cr-1Mo steel: An experimental and numerical study. *Fatigue & Fracture of Engineering Materials & Structures*, 47(5), 1677–1695. <https://doi.org/https://doi.org/10.1111/ffe.14267>
- Chandra, H. (2019). *Analisis Kegagalan Material*. UPT. Penerbit dan Percetakan.
- Chandra, H., Ammarullah, M. I., Marwani, M., Ellyanie, E., Warizal, W., Aditya, D., Pratiwi, D. K., & Utami, N. P. E. (2024). Preventing environmental and health problems due to LPG transport tank leaks: fatigue and crack behavior of heat-treated steel investigation. *Cogent Engineering*, 11(1). <https://doi.org/10.1080/23311916.2024.2304491>
- Darmo, S., Soenoko, R., Siswanto, E., & Widodo, T. D. (2018). Study on mechanical properties of pack carburizing SS400 steel with energizer pomacea canaliculata lamarck shell powder. *International Journal of Mechanical Engineering and Technology*, 9(5), 14–23. <https://doi.org/10.30574/ijeta.2022.11.2.0087>
- H. O. Fuchs, & Stephens, R. I. (1980). *Metal Fatigue In Engineering*. John Willey & Sons.
- Hafidz, M. D., & Chandra, H. (2023). *Karakteristik patah dan ketahanan lelah besi cor malleable*. 14(1), 307–315. <https://doi.org/10.21776/jrm.v14i1.1292>
- Humaidi, M. H., Suryono, A. F., & Hestiawan, H. (2022). *Pengaruh Variasi Arus Listrik Terhadap Nilai Kekerasan Hasil Lasan Baja ASTM A36 Variation Effect of Electrical Current on The Hardness Value of ASTM A36 Steel Welding* (Vol. 6, Issue 1).

<https://doi.org/10.33369/rekayasamekanika.v6i1.25451>

- Li, H. F., liu, Y. Q., Zhang, P., & Zhang, Z. F. (2023). A full-stage fatigue crack growth model for metallic materials. *International Journal of Fatigue*, 172, 107662. <https://doi.org/https://doi.org/10.1016/j.ijfatigue.2023.107662>
- Megyesy, E. F. (2008). *Pressure vessel handbook*. Pressure Vessel Pub.
- Moss, D., & Basic, M. (2013). *Pressure_Vessel_Design_Manual*. 1–832.
- Nugraha, H., Kusumaningtyas, I., & Miasa, I. M. (2022). Analisis Buckling dan Tegangan Bejana Tekan Horisontal pada Tekanan Kerja Eksternal. *Journal of Mechanical Design and Testing*, 4(2), 58. <https://doi.org/10.22146/jmdt.63592>
- Pineau, A., Benzerga, A. A., & Pardoën, T. (2016). Failure of metals I: Brittle and ductile fracture. *Acta Materialia*, 107, 424–483. <https://doi.org/https://doi.org/10.1016/j.actamat.2015.12.034>
- Pratowo, B., & Apriansyah, N. (2016). *Analisis Kekuatan Fatik Baja Karbon Rendah SC10 Dengan Tipe Rotary Bending*. 2, 49–58.
- Schneller, W., Leitner, M., Maier, B., Grün, F., Jantschner, O., Leuders, S., & Pfeifer, T. (2022). Artificial intelligence assisted fatigue failure prediction. *International Journal of Fatigue*, 155, 106580. <https://doi.org/https://doi.org/10.1016/j.ijfatigue.2021.106580>
- Siswanto, B., Teknik Mesin, J., Teknik, F., Wastukencana, S., & Cikopak No, J. (2021). *Jurnal Sustainable: Jurnal Hasil Penelitian dan Industri Terapan*. 10(01), 37–44.
- Suryana, D., Sani, A. A., & Sepriyanto, D. (2015). Pengaruh Dept of Cut Dan Feedrate Dengan Cutter Diameter 60 Mm Terhadap Kerataan Permukaan Material Astm a36 Pada Mesin Mitsubishi Cnc-Mill 3a. *Jurnal Austenit*, 7(April), 1–6. <https://doi.org/https://doi.org/10.5281/zenodo.4547522>
- Wciślik, W., & Lipiec, S. (2022). Void-Induced Ductile Fracture of Metals: Experimental Observations. In *Materials* (Vol. 15, Issue 18). MDPI. <https://doi.org/10.3390/ma15186473>
- Wirjosumarto, H., & Okumura, T. (2000). *Teknologi Pengelasan Logam*.